Supporting Information for:

Uncovering the molecular interactions in the catalytic loop that modulate the conformational dynamics in protein tyrosine phosphatase 1B

Danica S. Cui[1], James Michael Lipchock[2], Dennis Brookner[3], and J. Patrick Loria[1,3*]

AUTHOR ADDRESS [1]Department of Chemistry, Yale University, New Haven, CT, 06511

[2]Department of Chemistry, Washington College, Maryland

[3]Department of Molecular Biophysics and Biochemistry, Yale University, New Haven, CT 06511

Supplementary Tables

Table S1. Summary of residues experiencing $R_{ex} > 2\ s^{-1}$ obtained from the ^{13}C MQ CPMG relaxation dispersion experiments

	WT			T177A		P180A			F182A			P185A			P188A	
	Field (MHz)			Field (MHz)		Field (MHz)			Field (MHz)			Field (MHz)			Field (MHz)	
	600	800		600		600	700		600	700		600	800		600	700
	k_{ex}			k_{ex}		k_{ex}			k_{ex}			k_{ex}			k_{ex}	
	1920 ± 142			1910 ± 73		1460 ± 60			770 ± 110			775 ± 110			Group I: 1980 ± 60	Group II: 730 ± 110
2°	**Residues**		**2°**	**Residues**	**2°**	**Residues**		**2°**	**Residues**		**2°**	**Residues**		**2°**	**Residues**	
Q	261	261	Q	261	Q	261	261	Q	261	261	Q	261		Q	261	
WPD	184	184	WPD	184	WPD	184		α2'		23	α2'	19	19	WPD	184	184
P	219	219	P	219	P	219	219	α6		275	α2'	23		P	219	219
α2'	19	19	α2'	23	α5	246					α5	246	246	α6	281	
α2'	23	23	α5	246	α6	281	281				α6	281	281	β2	72	72
α5	246	246	α6	281	β1		57				β1	57		α2'	23	23
α6	275	275	β2	72	β2	72	72							α5	246	
α6	281	281	β11	171	β11	171								α6	275	275
β1	57	57														
β7	134	134														

Table S2. Data collection and refinement statistics of PTP1B Ala loop mutants

	T177A apo	P180A apo	F182A apo	P185A apo	P188A apo
PDB ID	6PFW	6OMY	6OL4	6OLV	6OLQ
Data collection					
X-ray source	Home source	Home source	Home source	Home source	Home source
Wavelength (Å)	1.54	1.54	1.54	1.54	1.54
Space group	P 3_1 2 1	P 3_1 2 1	P 3_1 2 1	P 3_1 2 1	P 3_1 2 1
Cell dimensions					
a, b, c (Å)	87.93 87.93 102.92	88.26 88.26 103.32	88.09 88.09 103.74	88.52 88.52 103.87	88.52 88.52 104.25
α, β, γ (º)	90 90 120	90 90 120	90 90 120	90 90 120	90 90 120
Resolution range	35.71 - 2.34 (2.42 - 2.34)	31.4 - 2.11 (2.18 - 2.11)	30.73 - 2.15 (2.23 - 2.15)	38.33 - 2.10 (2.18 - 2.10)	33.74 - 2.1 (2.18 - 2.1)
R-merge	0.086 (0.807)	0.079 (0.173)	0.108 (0.727)	0.114 (0.632)	0.076 (0.236)
Mean I/sigma(I)	11.1 (2.3)	22.4 (13.9)	11.4 (3.0)	10.3 (3.9)	16.6 (7.8)
Total reflections	112123 (10036)	289922 (26583)	251738 (21529)	295778 (27287)	193332 (17197)
CC1/2	0.998 (0.878)	0.998 (0.990)	0.998 (0.885)	0.999 (0.889)	0.997 (0.975)
Completeness (%)	92.9 (96.0)	98.1 (99.3)	96.2 (99.3)	98.7 (99.8)	97.7 (99.2)
Multiplicity	5.9 (5.3)	10.7 (10.3)	9.8 (8.6)	10.6 (10.0)	6.9 (6.3)
Refinement					
Unique reflections	18473 (1885)	27154 (2652)	24828 (2505)	27591 (2723)	27420 (2728)
Wilson B-factor	39.14	29.29	38.93	33.11	30.09
Reflections used in refinement	18471 (1885)	27152 (2696)	24823 (2505)	27586 (2723)	27415 (2728)
R-work	0.209 (0.282)	0.187 (0.222)	0.217 (0.286)	0.206 (0.249)	0.203 (0.2376)
R-free	0.247 (0.368)	0.203 (0.284)	0.258 (0.349)	0.237 (0.345)	0.235 (0.3058)
Number of non-hydrogen atoms	2555	2688	2782	2549	2768
macromolecules	2410	2437	2593	2301	2521
ligands	16	12	18	22	22
solvent	129	239	171	226	225
Protein residues	297	297	296	283	297
Average B-factor	42.05	32.66	46.12	39.12	34.39
macromolecules	41.86	31.84	45.93	38.39	33.68
ligands	60.72	42.77	60.42	54.60	43.16
solvent	43.36	40.46	47.61	45.01	41.52
RMS(bonds)	0.010	0.009	0.009	0.011	0.011
RMS(angles)	1.07	0.97	1.03	1.02	1.16
Ramachandran favored (%)	96.27	97.29	96.56	96.09	96.95
Ramachandran allowed (%)	3.39	2.37	3.09	3.56	2.71
Ramachandran outliers (%)	0.34	0.34	0.34	0.36	0.34

Table S3. Data collection and refinement statistics for vanadate soaked structures

	T177A Vanadate	P180A Vanadate	F182A Vanadate	P185A Vanadate	P188A Vanadate
PDB ID:	6PGT	6PM8	6PHA	6PHS	6PGO
Data collection					
X-ray source	Home source	Home source	Home source	Home source	Home source
Wavelength (Å)	1.54	1.54	1.54	1.54	1.54
Space group	P 3_1 2 1	P 3_1 2 1	P 3_1 2 1	P 3_1 2 1	P 3_1 2 1
Cell dimensions					
a, b, c (Å)	88.08 88.08 103.65	88.30 88.30 104.00	87.56 87.56 102.37	87.70 87.70 102.96	88.23 88.23 104.07
α, β, γ (º)	90 90 120	90 90 120	90 90 120	90 90 120	90 90 120
Resolution range	38.14 - 2.20 (2.38 - 2.20)	28.90 - 2.06 (2.18 - 2.06)	30.47 - 2.30 (2.38 - 2.30)	37.98 - 2.13 (2.25 - 2.13)	30.79 - 2.10 (2.18 - 2.10)
R-merge	0.086 (0.335)	0.094 (0.310)	0.215 (1.004)	0.109 (0.728)	0.062 (0.214)
Mean I/sigma(I)	16.9 (7.2)	16.4 (6.8)	4.4 (2.7)	10.0 (2.4)	17.7 (8.3)
Total reflections	220924 (21380)	289255 (26078)	195928 (18013)	144125 (14177)	183285 (15601)
CC1/2	0.998 (0.980)	0.998 (0.975)	0.992 (0.851)	0.997 (0.805)	0.998 (0.974)
Completeness (%)	96.1 (98.2)	98.3 (98.2)	97.9 (99.9)	99.5 (98.4)	95.1 (98.6)
Multiplicity	10.5 (10.2)	10.5 (9.8)	9.5 (8.9)	5.8 (5.8)	6.8 (5.8)
Refinement					
Unique reflections	23137 (2296)	29002 (2683)	20246 (2032)	26023 (2535)	26477 (2689)
Wilson B-factor	32.78	29.65	37.61	34.03	30.65
Reflections used in refinement	23133 (2040)	29000 (2685)	20243 (2032)	26020 (2437)	26475 (2689)
R-work	0.189 (0.324)	0.195 (0.243)	0.223 (0.246)	0.199 (0.267)	0.195 (0.226)
R-free	0.230 (0.336)	0.220 (0.270)	0.276 (0.335)	0.242 (0.287)	0.225 (0.297)
Number of non-hydrogen atoms	2708	2730	2616	2555	2683
macromolecules	2435	2432	2417	2410	2416
ligands	23	23	47	17	28
solvent	250	275	152	128	239
Protein residues	298	297	297	297	297
Average B-factor	36.40	32.60	36.53	37.32	33.92
macromolecules	35.79	31.57	35.81	36.97	33.21
ligands	42.47	41.38	51.17	45.30	44.48
solvent	41.75	40.97	43.53	42.92	39.80
RMS(bonds)	0.010	0.017	0.010	0.009	0.010
RMS(angles)	1.24	1.03	1.14	1.11	1.04
Ramachandran favored (%)	96.96	96.95	96.95	97.29	96.95
Ramachandran allowed (%)	2.70	2.71	2.71	2.03	2.71
Ramachandran outliers (%)	0.34	0.34	0.34	0.68	0.34

Statistics for the highest-resolution shell are shown in parentheses.

Supplementary Figures

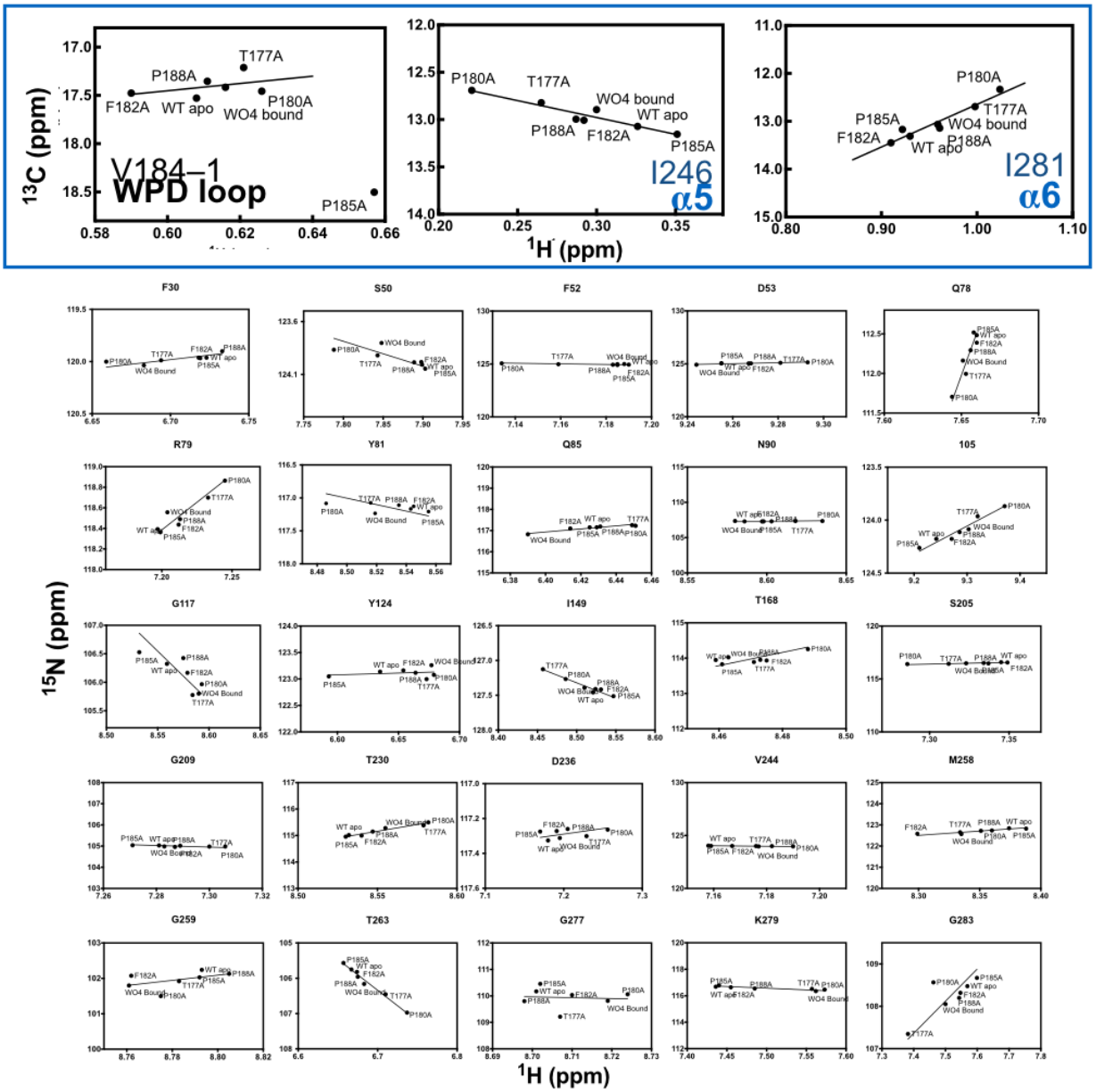

Fig. S1.

Examples of linear distribution of ^{13}C (top blue box) and ^{15}N chemical shift in allosteric regions of PTP1B due to alanine WPD loop mutants. The mutants represent varying degrees of open and closed WPD loop equilibrium. Apo WT (97% open) and WO_4^{2-} bound (37% closed) chemical shifts are shown for reference.

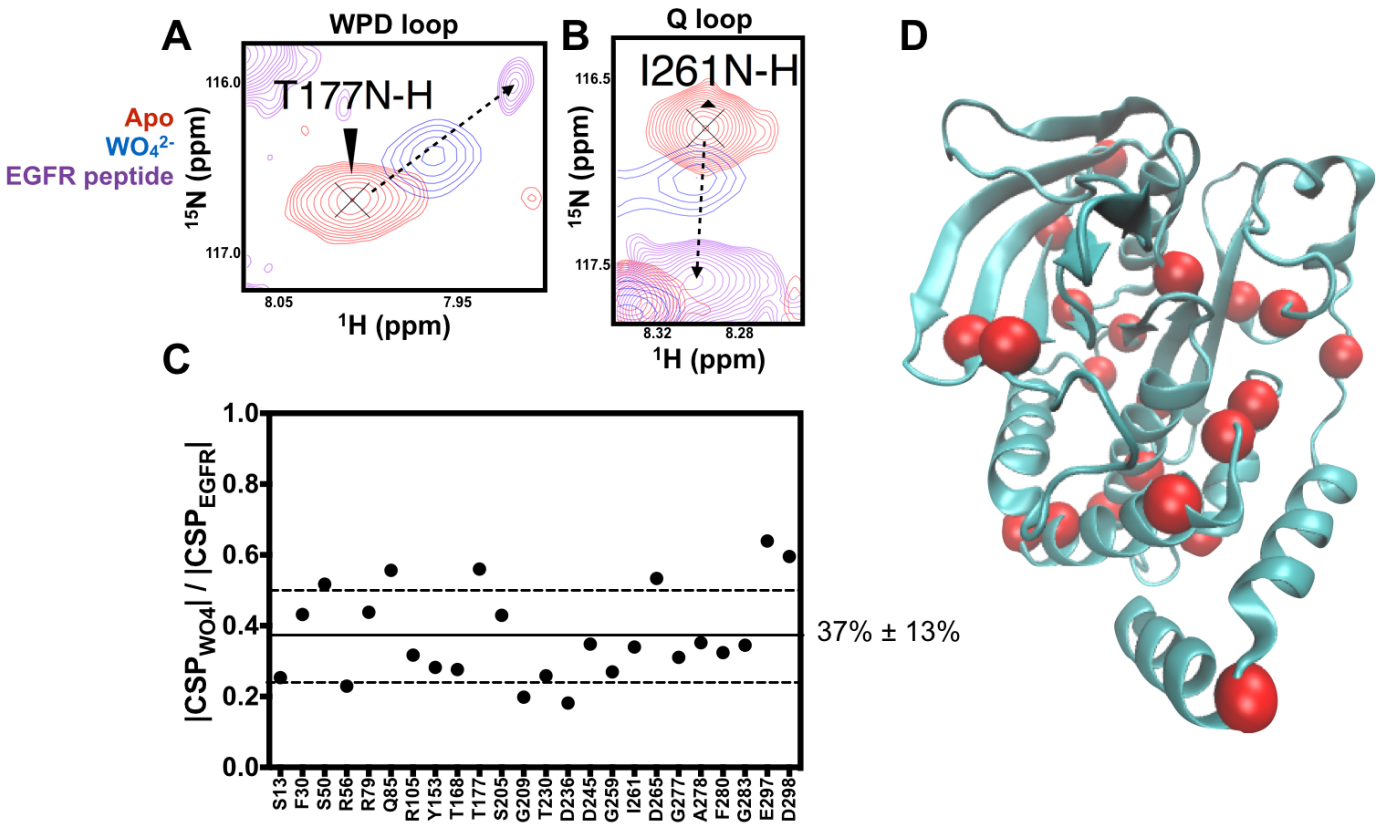

Fig. S2.

The closed population of WO_4^{2-} bound PTP1B is estimated through the comparison to NMR chemical shifts of DADEXLIP (EGFR) peptide saturated PTP1B. An overlay of WT apo (red), WO_4^{2-} (blue), and EGFR peptide (purple) saturated PTP1B ^{15}N spectra is shown for A) T177 (WPD loop) and B) I261 (Q-loop). The CSPs of WO_4^{2-} are observed to lie along a linear trajectory between WT apo and EGFR peptide bound resonances. This indicates that upon binding, both ligands shift the two–state protein conformational equilibrium from open to closed state albeit to varying degrees. C) Plot of the ratio of CSP magnitudes between WO_4^{2-} and EGFR for all residues that exhibit a linear CSP trend. The CSP induced by EGFR peptide binding occurs in the slow exchange regime. The EGFR peptide bound resonance observed for each residue will reflect protein in the closed conformation. The ratio of CSP_{WO4}/CSP_{EGFR} estimates the closed population of WO_4^{2-} bound to be 37% ±13%. D) Cartoon representation of PTP1B with the residues used for CSP analysis shown as red spheres.

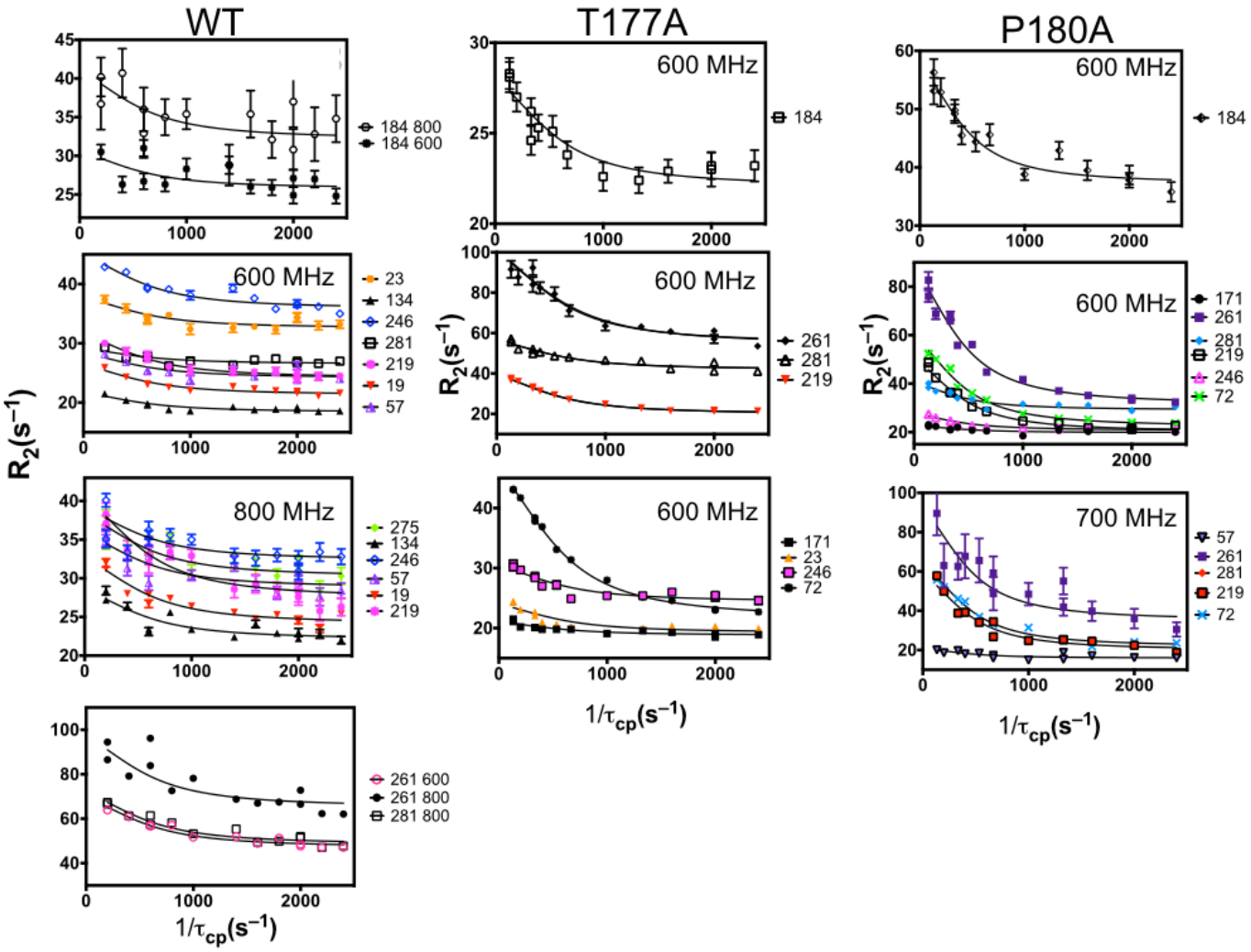

Fig. S3.

^{13}C MQ CPMG relaxation dispersion curves for WT, T177A, and P180A are shown for residues exhibiting $R_{ex} > 2s^{-1}$. Data were acquired at 600, 700, and 800 MHz.

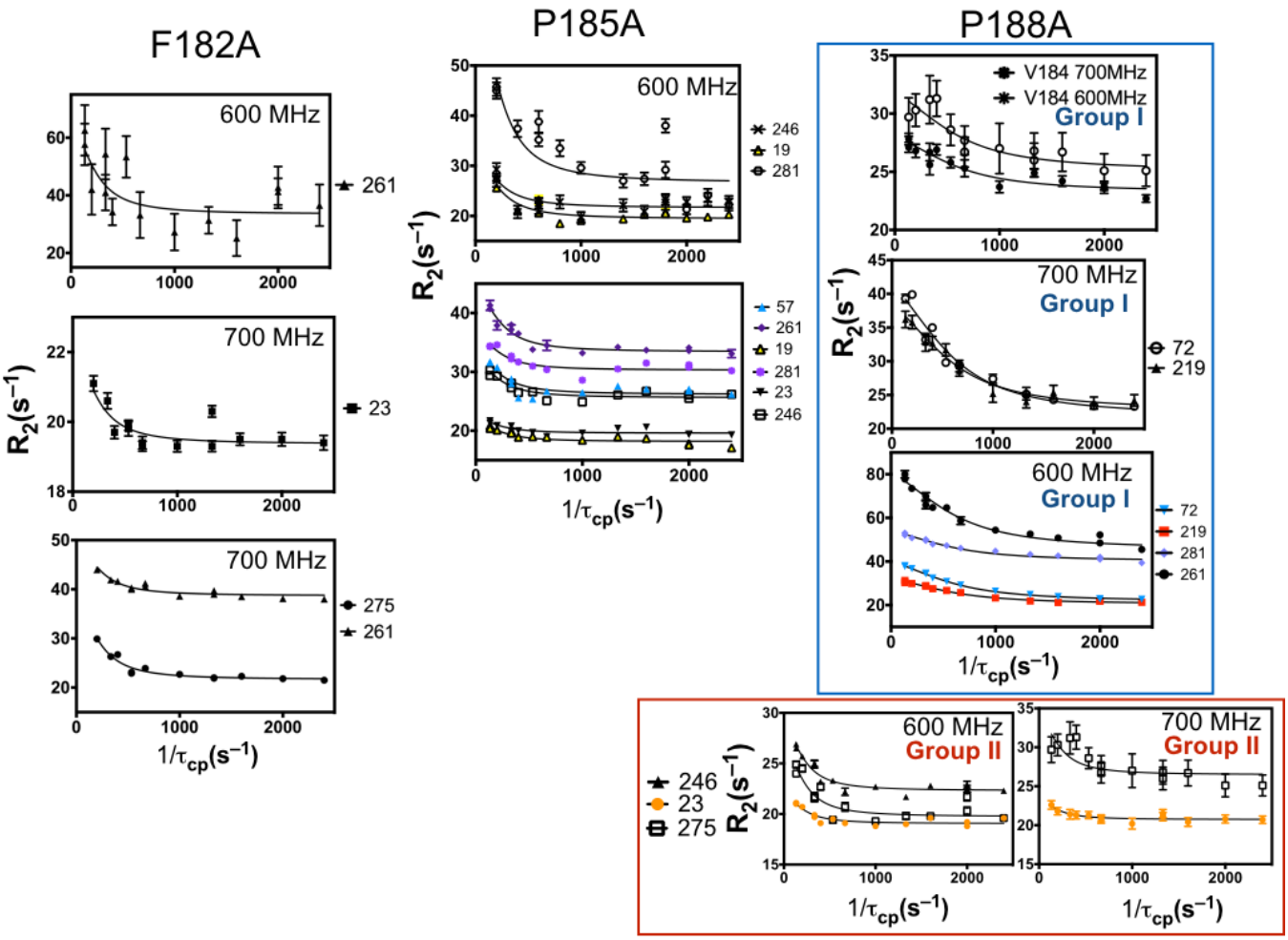

Fig. S4.

^{13}C MQ CPMG relaxation dispersion curves for F182A, P185A, and P188A are shown for residues exhibiting $R_{ex} > 2s^{-1}$. For P188A blue and red boxes denote residue grouping of fast (1980 s^{-1}) and slow (730 s^{-1}) timescale motions. Data were acquired at 600, 700, and 800 MHz.

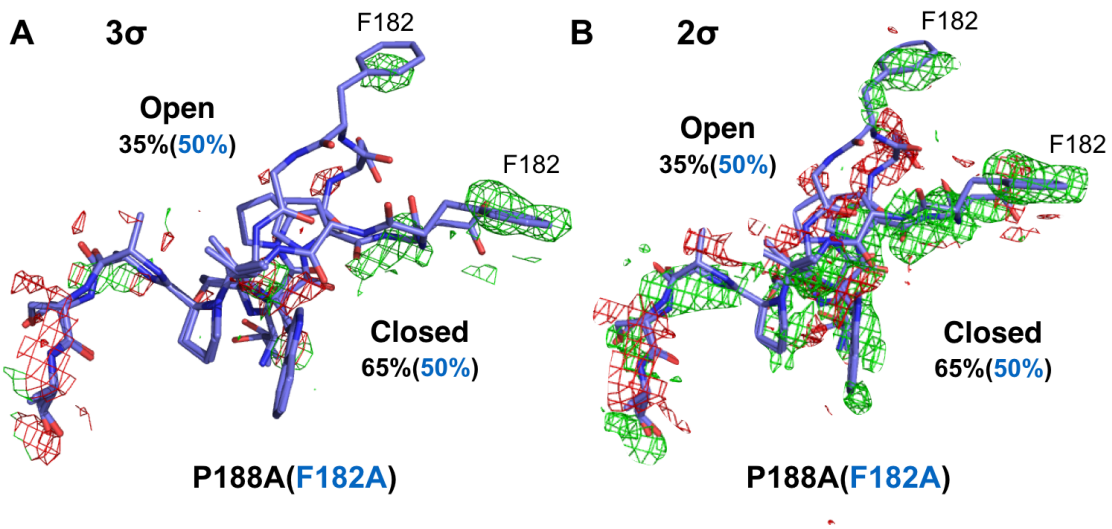

Fig. S5.

Fo – Fo isomorphous difference map of P188A – F182A. This is used to validate the occupancy modeling of the electron density in the open and closed WPD loop conformations. P188A has an open:closed occupancy of 35:65%, while F182A has an occupancy of 50:50%. Here we show the difference map at A) +/- 3σ and B) +/- 2σ . The positive peaks are shown in green, negative peaks are shown in red. At 3σ, the missing density for the aromatic side chain in F182A is apparent. At 2σ, differences in electron density between P188A, and F182A in the open and closed states become apparent. In the closed conformation, the difference map reveals positive peaks indicating that there is more electron density in the closed conformation in P188A relative to F182A. In the open loop conformation, the Fo-Fo map shows negative density demonstrating that there is more electron density the open loop of F182A than P188A. The difference map is rendered in Pymol[1] and projected on to the WPD loop (177-188) of P188A.

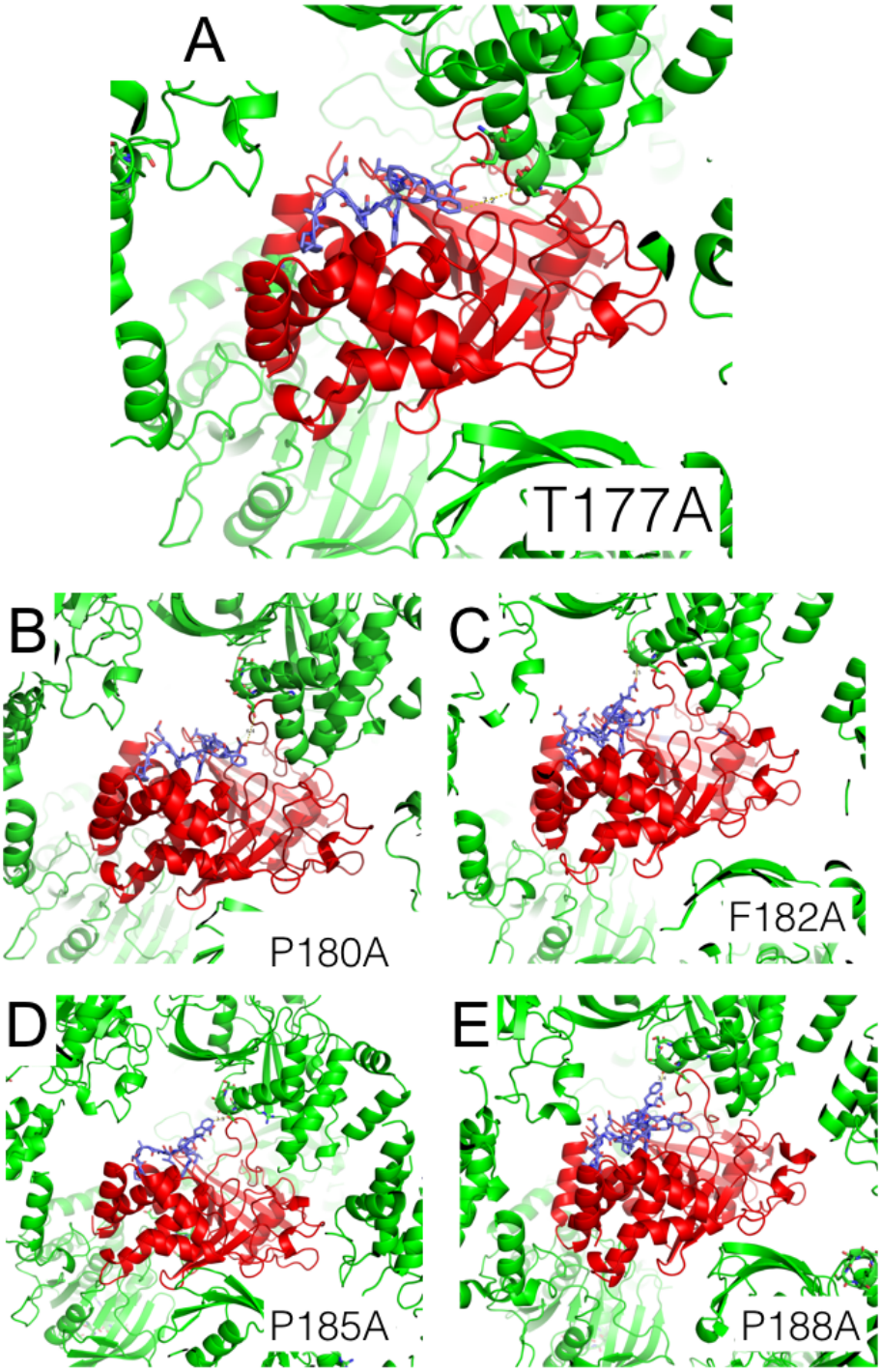

Fig. S6.

Crystal packing in PTP1B Ala loop mutants. Symmetry molecules observed in the asymmetrical unit. The molecule of interest is shown in red. The symmetry molecules are represented in green. The WPD loop is shown in stick (blue).

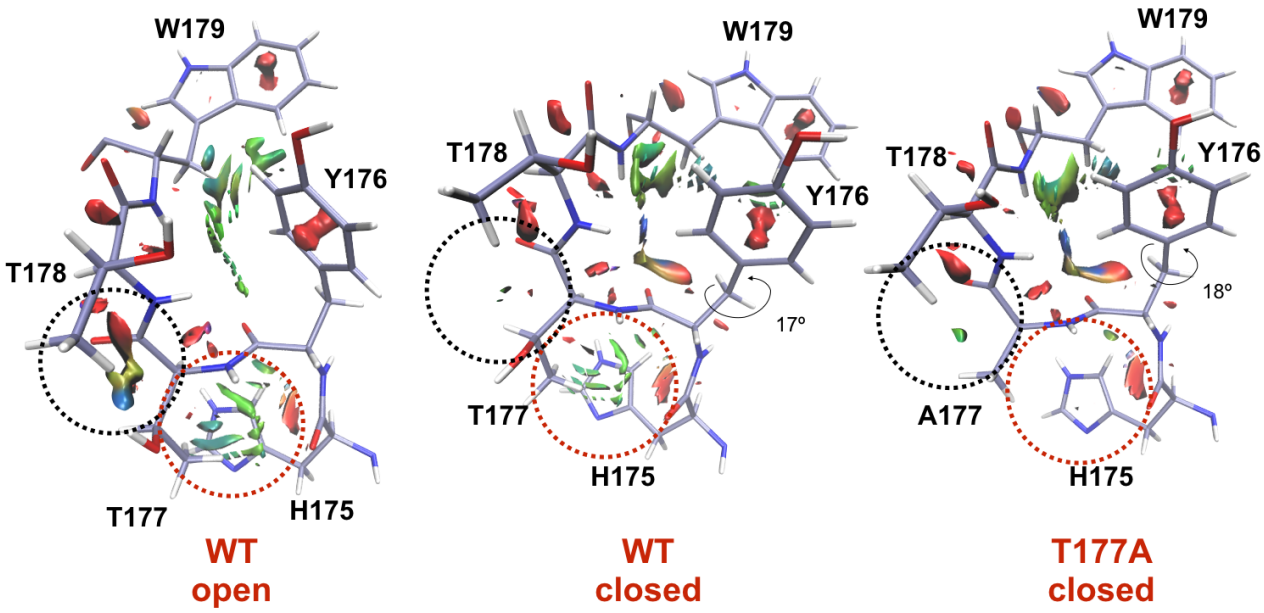

Fig. S7.

Comparison of interactions between H175 to T178 in WT and T177A using NCIplot.[2] The reduced density gradient surfaces are rendered using isosurface in VMD[3] with an isovalue = 0.4 au. A BGR color scale is used to describe the attractive (blue), van der Waals (green), and repulsive (red) interactions. The color scale is set between a scale of $-2 < \text{sign}(\lambda 2)\rho < 2$. The dashed enclosures represent the main differences between mutant and WT.

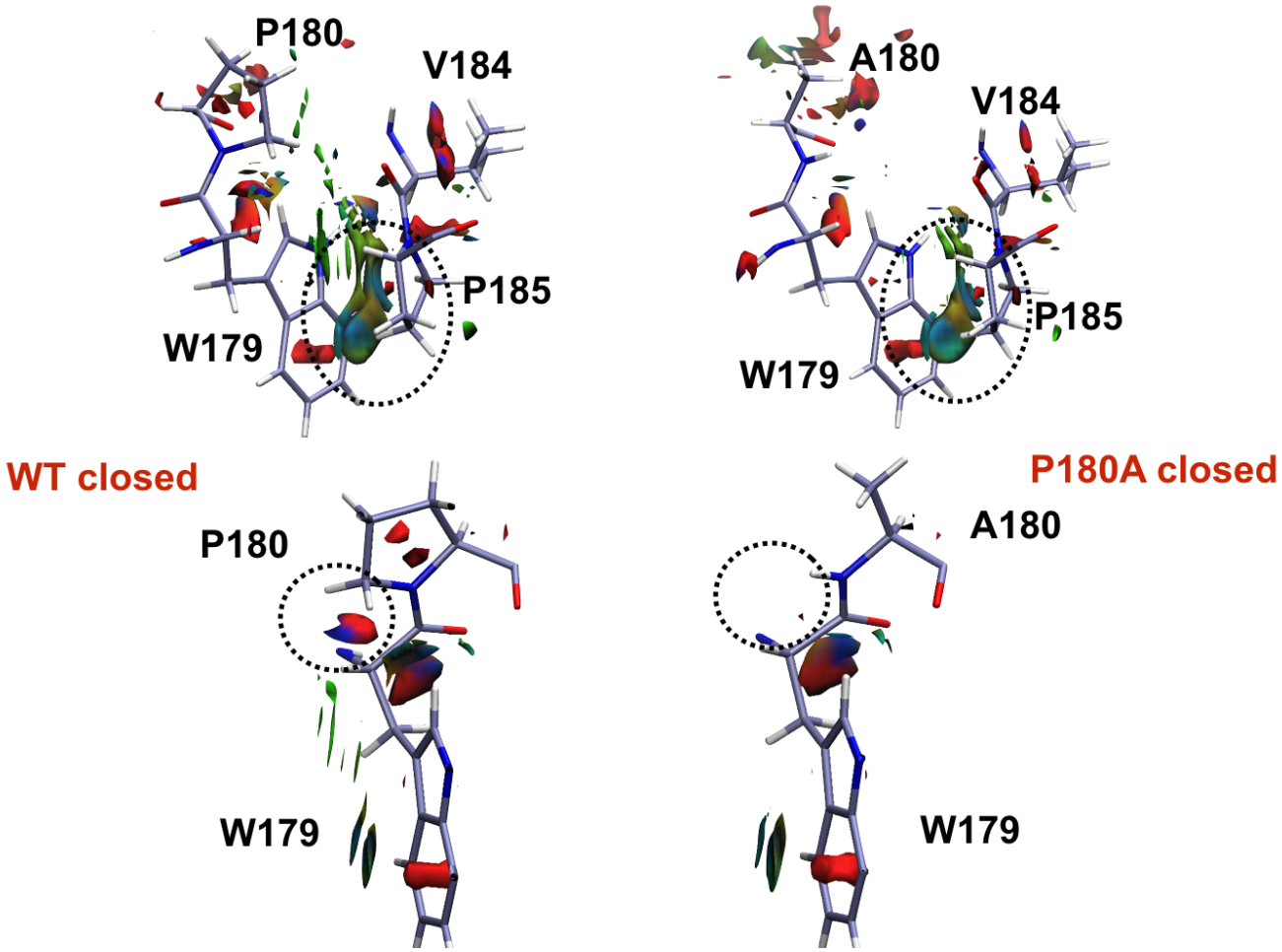

Fig S8.
Comparison of the closed loop interactions in WT (left) and P180A (right). CH-π interaction between W179 and P185 is retained in P180A. Additionally, there is less side chain steric repulsion observed between the side chain of W179 and A180 compared to P180. The dashed enclosures represent the main differences between mutant and WT.

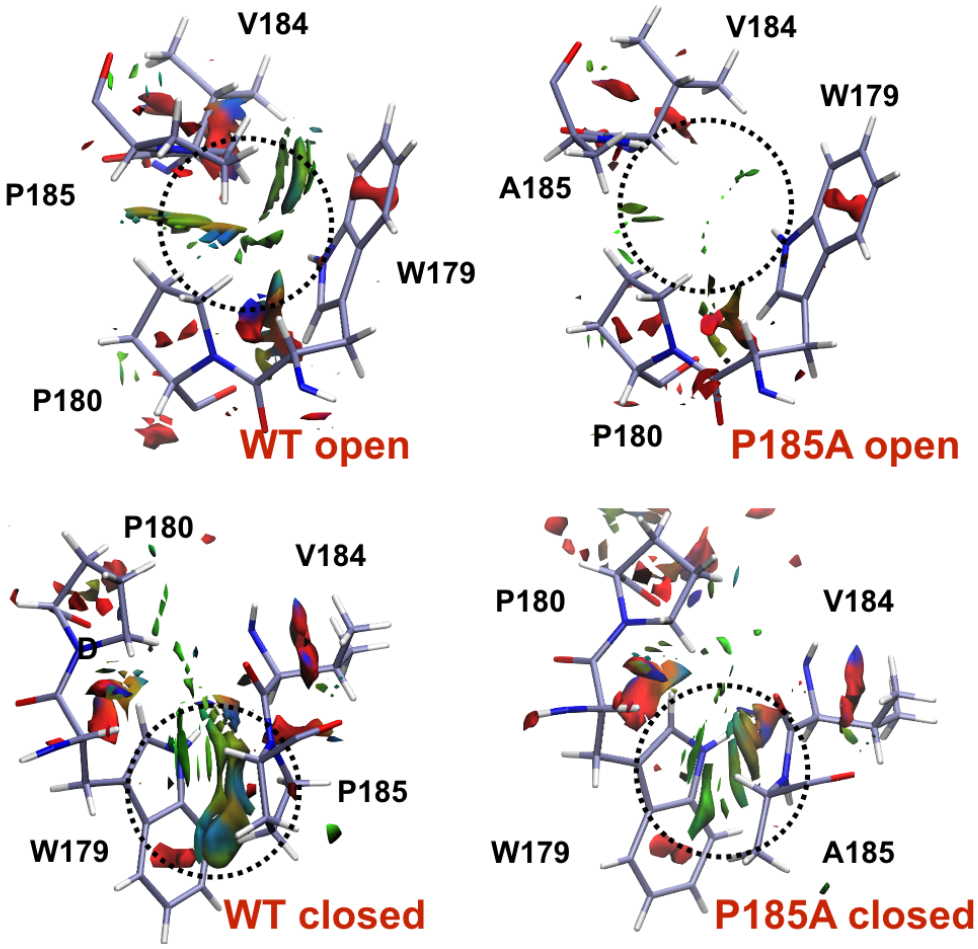

Fig. S9.

Molecular rendering of W179, P180, V184, P185 (A185) in open conformations of WT (A) and P185A (B), and closed conformations of WT (C) and P185A (D). NCIplot was used to visualize the van der Waals interactions and CH-π interactions in the open and closed states. There is a decrease in side chain interactions formed by A185 in both the open and closed loop states compared to WT. The dashed enclosures represent the main differences between mutant and WT.

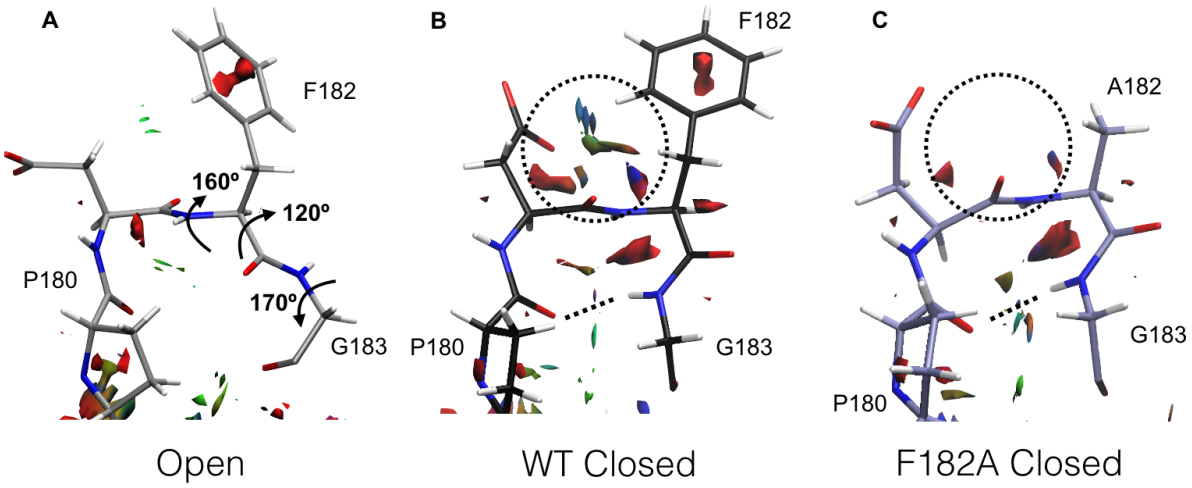

Fig. S10.

A) Rotation of ψ and φ angle in 182 and 183 are shown on the open WT loop structure. B) Closed WT loop structure with steric hindrance indicated by the red arrows. C) F182A loop closed structure with steric interactions mapped. H-bond between P180 and G183 is represented with a dashed line. The dashed enclosures represent the main differences between mutant and WT.

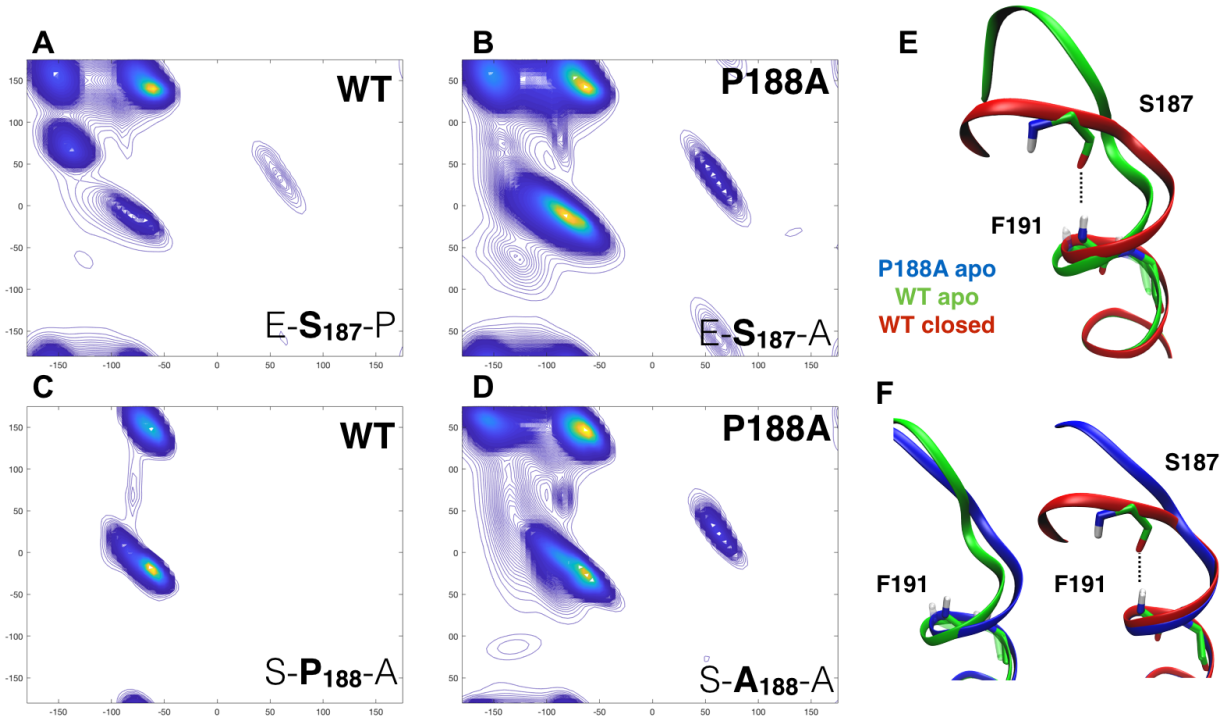

Fig. S11.
Probability distribution of neighbor dependent Ramachandran plots[4,17] for A) S187 (WT), B) S187 (P188A), C) P188 (WT), and D) A188(P188A). E) Changes in backbone of α3 between open (green) and closed (red) WT loop is shown in ribbon. Amide of F191 is shown in stick for open (transparent) and closed states. F) Comparison of WT open and closed states in α3 to P188A apo (blue) and the amide position of F191.

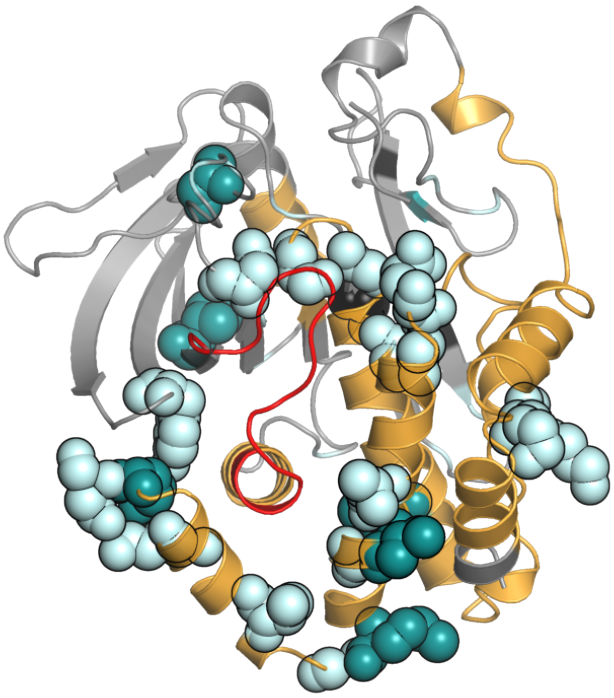

Fig. S12.
Allosteric network identified through frequency analysis of CSP of 13 Ala WPD loop mutations. [5] Dα is represented in orange, Dβ in gray, and the WPD loop is in red. Residues that are allosterically coupled to the active site are shown in teal(> 7 out of 13 loop mutants) and light blue (>5 out of 13 loop).

References

[1] In *The PyMOL Molecular Graphics System, Version 2.0 Schrödinger, LLC.*

[2] Contreras-Garcia, J., Johnson, E. R., Keinan, S., Chaudret, R., Piquemal, J. P., Beratan, D. N., and Yang, W. (2011) NCIPLOT: a program for plotting non-covalent interaction regions, *J Chem Theory Comput 7*, 625-632.

[3] Humphrey, W., Dalke, A., and Schulten, K. (1996) VMD: visual molecular dynamics, *J Mol Graph 14*, 33-38, 27-38.

[4] Ting, D., Wang, G., Shapovalov, M., Mitra, R., Jordan, M. I., and Dunbrack, R. L., Jr. (2010) Neighbor-dependent Ramachandran probability distributions of amino acids developed from a hierarchical Dirichlet process model, *PLoS Comput Biol 6*, e1000763.

[5] Cui, D. S., Beaumont, V., Ginther, P. S., Lipchock, J. M., and Loria, J. P. (2017) Leveraging Reciprocity to Identify and Characterize Unknown Allosteric Sites in Protein Tyrosine Phosphatases, *J Mol Biol 429*, 2360-2372.